

# Investigation on Control Issues in Power Converters for Advanced Micro-Grid Operations

Tsao-Tsung Ma

**Abstract** This paper investigates a novel design concept, in which a hybrid power interface system (HPIS) is constructed to work smartly in various micro-grid (MG) operations. Some distributed generation (DG) systems, e.g. the wind turbine generator (WTG) and the photovoltaic (PV) systems conventionally generate real power based on natural conditions thus the average utilization rate of the entire asset is normally low. To eliminate this shortcoming, the proposed HPIS aims to use the DG inverter system optimally. To achieve a cost-effective design, the modular design concept and the related droop control algorithms are incorporated into the proposed HPIS to maximize its operating capability in terms of real power regulation, active power filter (APF) functions for current harmonics compensation and reactive power compensator for MG voltage support and power factor correction. The HPIS is designed to fully utilize the DG inverter capacity after performing various real power control functionalities required by the system operator. In this paper, the mathematical model of HPIS and its related controllers designed in two-axis reference frame are firstly addressed. Then, simulation studies on a simplified MG network are carried out in the Matlab/Simulink software environment. Typical results are presented with brief discussions to demonstrate the feasibility and performances of the proposed control schemes.

**Keywords** Active power filter (APF) · Distributed generator (DG) · Hybrid power interface system (HPIS) · Micro-grid (MG) · Photovoltaic (PV) · Wind turbine generator (WTG)

---

T.-T. Ma (✉)

Department of Electrical Engineering, National United University,  
No.1, Lien-Da, Kung-Ching Li, Miao-Li city 36003, Taiwan R.O.C  
e-mail: tonyma@nuu.edu.tw

## 1 Introduction

The rapid development of distributed generation (DG) and micro-grid (MG) systems is an inevitable trend; however, with the addition of these new generation units the conventional distribution network has to face many new challenges in terms of system operation, protection, optimization and stability problems. In recent years, renewable energy resources (RES) based distributed power generations (DG), micro-grids (MG) and state-of-the-art communication and control technologies have been recognized to play important roles in the achievement of some energy policies set by Taiwan's government. The goal of these energy policies include reductions in high-polluting power generations and global greenhouse gas emissions, improved diversity and security of energy supply and the exploitation of possible incentives for creating local value added opportunities for the related industrial sectors in Taiwan. Based on the related technical reports in the open literature, potential RES based power generations may include wind turbine generator (WTG) [1], photovoltaic (PV) [2], and fuel cell (FC) [3]. Of these power generating methods, the interests in PV energy is growing worldwide over last ten years. Although the PV generation system is still expensive, according to recent published reports, PV prices have dropped by 45 % over last two years and further drop is expected in the near future [4]. In fact, a number of different PV incentive programs have been introduced in Taiwan since 2008. With the same objectives, some of the developed countries are currently promoting residential and commercial uses of PV generation systems [5–7]. Based on the standards such as IEEE1547, IEEE 929 and UL1741, PV inverter systems should operate at unity power [8]; however, this regulation has some limitations in practical applications. It has been proved that with proper design of the controllers these inverter systems working as the power interfaces in WTG, PV and FC all have the capability to provide additional control functions in addition to the regulation of real power generated from the RES. Intrinsically, some DG systems, e.g. the wind turbine generator and the PV system generate real power based on practical conditions thus the average utilization rate of the entire asset is normally low. This has resulted in that the payback time period for the system owners becomes longer. To make the best use of the DG hardware systems, the concept of utilizing PV inverter as a reactive power controller during the night time for voltage control thereby increasing the connectivity of a nearby wind farm, is proposed in [9]. A number of potential operations of a 3-phase PV grid connected inverter are discussed in [10, 11]. Some similar examples regarding reactive power compensation and voltage support in MG are also illustrated in [12, 13]. However, in the above published papers, only individual control function has been included in the operation of DG inverters. This paper investigates a novel design concept concerning the feasibility of performing multiple control functions in the DG inverter system working in micro-grids. To achieve a cost-effective design, the modular design concept is considered in the proposed HPIS to maximize the operating capability of DG inverter. With the proposed design concept the DG inverter is able to optionally utilize the unused portion of rated capacity after performing the function of real power generation.

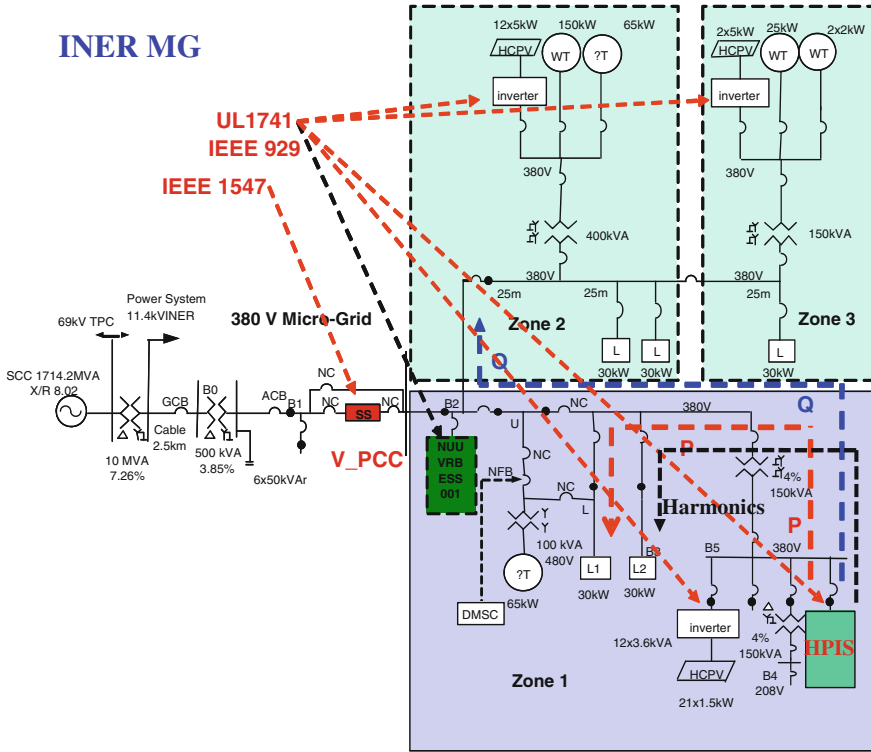


Fig. 1 System diagram of a typical micro-grid with various DG inverters (Taiwan)

## 2 The First Micro-Grid Test Bed in Taiwan

Distribution systems possessing DGs and controllable loads with the ability to operate in both grid-connected and standalone modes are an important class of the so-called MG power systems [14–16]. A typical MG system constructed by the Institute of Nuclear Energy Research (INER) in Taiwan is shown in Fig. 1 [17]. As can be seen in Fig. 1, the INER micro-grid with a designed maximum capacity of 475.5 kVA has three independent Zones. In Zone1, there is a 31.5 kVA PV, a 65 kVA microturbine, a total of 60 kVA controllable load bank, a 150 kVA wind turbine and a 100 kVA ABB PCS-100 BESS. Zone2 has a 60 kVA PV system, a 65 kVA microturbine and a total of 60 kVA controllable load bank. Zone3 is equipped with a 4 kW small wind turbine, a 25 kVA wind turbine, a 10 kVA PV, a 65 kVA microturbine and a 30 kVA controllable load bank. To facilitate possible tests considering the conditions of practical operating modes, Zone 2 and Zone 3 are connected in series, while Zone 1 and Zone 2 are in parallel.

It is well known that MG strives for optimized operation of the aggregated distribution systems by coordinating the various DGs, ESS and load resources not only when connected to the distribution system but also in a standalone mode. In either modes of operation, advanced local controls, energy management, power quality and protection technologies are required for robustness and reliability. In practice, the energy management optimization objective function can be tailored to the needs of each application. In a practical MG project, the overall objective is to optimize operating performance and cost in the normally grid-connected mode, while ensuring that the system is capable of meeting the performance requirements in standalone mode. To satisfy the needs of possible applications, some ESS units are inevitably required. In the INER MG project, two ESS are to be installed to achieve some advanced operations and power management functions.

### **3 Modular HPIS Principles and Control Schemes**

#### ***3.1 HPIS Hardware Configuration***

The operating principles and control concepts of the proposed HPIS are actually derived from the static synchronous compensator, a popular shunt-type FACTS device. In this paper, a basic HPIS hardware configuration which consists of a 3-phase switching converter using 6 IGBT switches and a three-phase power grid model, as shown in Fig. 2 is chosen to introduce the proposed HPIS operating principles and its control schemes. The IGBT converter in the HPIS is designed to be operated from a DC link voltage provided by a PV or any kind of RES. In normal operations, the active power can be controlled in either direction between the AC terminals of the converter and the grid to regulate the DC voltage and thus the real power generation of the DG. In this hardware topology, the converter can also generate or absorb reactive power independently at its AC output terminals to act as a reactive power generator or an APF.

In practical applications, two or more HPIS might be needed to work in parallel to meet the system operating requirement. Therefore, implementing effective control over P and Q is very important from the operational and control points of view. Figure 3 shows the system block diagram of a two HPIS modules working in parallel. Of the feasible control schemes, the droop control method has been widely used for controlling the parallel connected DG inverters. In this case, the inverters are controlled in such a way that the amplitude and frequency of the reference voltage signal will follow a droop as the load current increases and these droops are used to allow independent HPIS to share the load in proportion to their capacities.

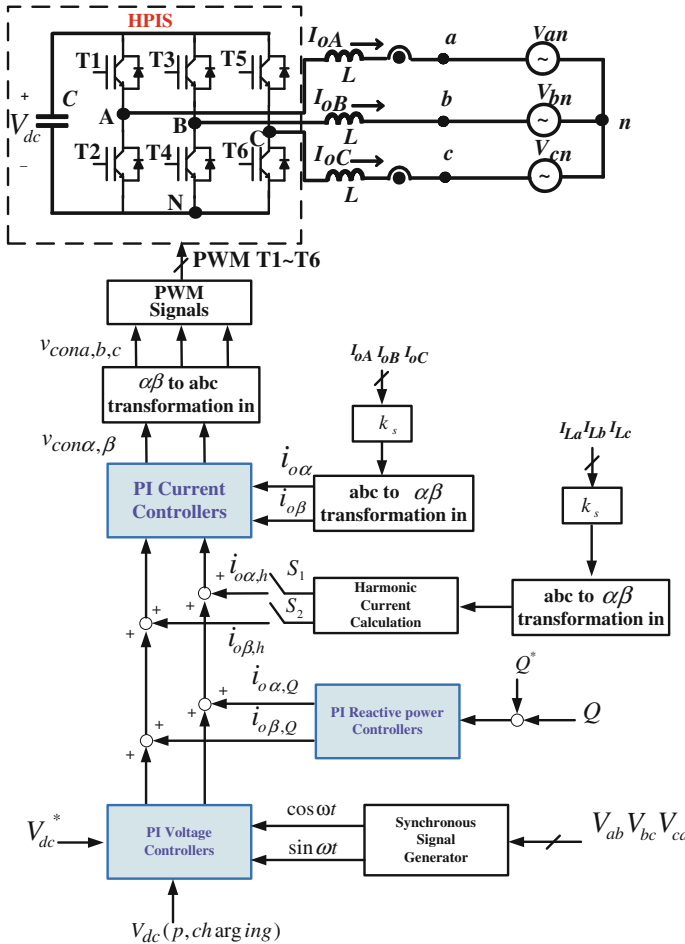
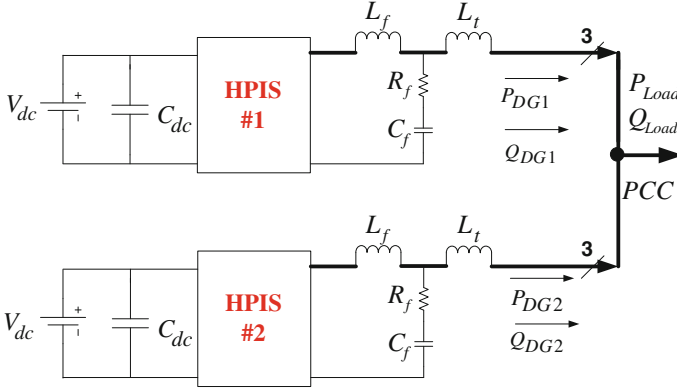


Fig. 2 Simplified MG model with the proposed HPIS and control signals

## 4 Design of HPIS Control Systems

In this paper, three important control functions are designed for the HPIS; i.e. real power regulation for DG, reactive power compensation for the grid and harmonic currents compensation for the local nonlinear load. These control functions can be activated simultaneously or individually. Because the proposed compensating requirements, i.e. real and reactive power or harmonic compensation, are directly related to the current control, shunt-type connection of DG inverter is a realistic topology as it normally injects currents at PCC. Therefore, this study uses the shunt-type connecting format for the implementation of HPIS control system shown in Fig. 2. With a number of mathematical manipulations, the output voltages and cur-



**Fig. 3** The system block diagram of a two HPIS modules working in parallel

rent commands of the HPIS can be obtained in two-axis reference frame as briefly addressed below. From Fig. 2, the following voltage and current equations can be easily obtained on KVL.

$$\begin{cases} L \frac{dI_{oA}}{dt} = V_{AN} - V_{an} - V_{nN} \\ L \frac{dI_{oB}}{dt} = V_{BN} - V_{bn} - V_{nN} \\ L \frac{dI_{oC}}{dt} = V_{CN} - V_{cn} - V_{nN} \end{cases} \quad (1)$$

The above (1) can be rewritten into (2) and the equivalent forms in the stationary reference frame as expressed in (3) and (4).

$$\begin{bmatrix} L \frac{dI_{oA}}{dt} \\ L \frac{dI_{oB}}{dt} \\ L \frac{dI_{oC}}{dt} \end{bmatrix} = \frac{2}{3} \begin{bmatrix} 1 & -\frac{1}{2} & -\frac{1}{2} \\ -\frac{1}{2} & 1 & -\frac{1}{2} \\ -\frac{1}{2} & -\frac{1}{2} & 1 \end{bmatrix} \left( \begin{bmatrix} V_{AN} \\ V_{BN} \\ V_{CN} \end{bmatrix} - \begin{bmatrix} V_{an} \\ V_{bn} \\ V_{cn} \end{bmatrix} \right) \quad (2)$$

$$\begin{bmatrix} L \frac{dI_{o\beta}}{dt} \\ L \frac{dI_{o\alpha}}{dt} \end{bmatrix} = k_{pwm} \begin{bmatrix} 1 & 0 \\ 0 & 1 \end{bmatrix} \begin{bmatrix} v_{con\beta} \\ v_{con\alpha} \end{bmatrix} - \begin{bmatrix} 1 & 0 \\ 0 & 1 \end{bmatrix} \begin{bmatrix} v_{s\beta} \\ v_{s\alpha} \end{bmatrix} \quad (3)$$

$$\begin{bmatrix} I_{o\beta} \\ I_{o\alpha} \end{bmatrix} = \frac{k_{pwm}}{sL} \begin{bmatrix} 1 & 0 \\ 0 & 1 \end{bmatrix} \begin{bmatrix} v_{con\beta} \\ v_{con\alpha} \end{bmatrix} - \frac{1}{sL} \begin{bmatrix} 1 & 0 \\ 0 & 1 \end{bmatrix} \begin{bmatrix} v_{s\beta} \\ v_{s\alpha} \end{bmatrix} \quad (4)$$

Finally, the three-phase output current signals for the HPIS can be directly derived from (4) by using the inverse Clarke's transformation. In the open literature, many current control methods for three phase inverter systems have been proposed. Among them, a PWM based control scheme using high-frequency switching has been widely used in many applications. This is due to the fact that the design of output filter

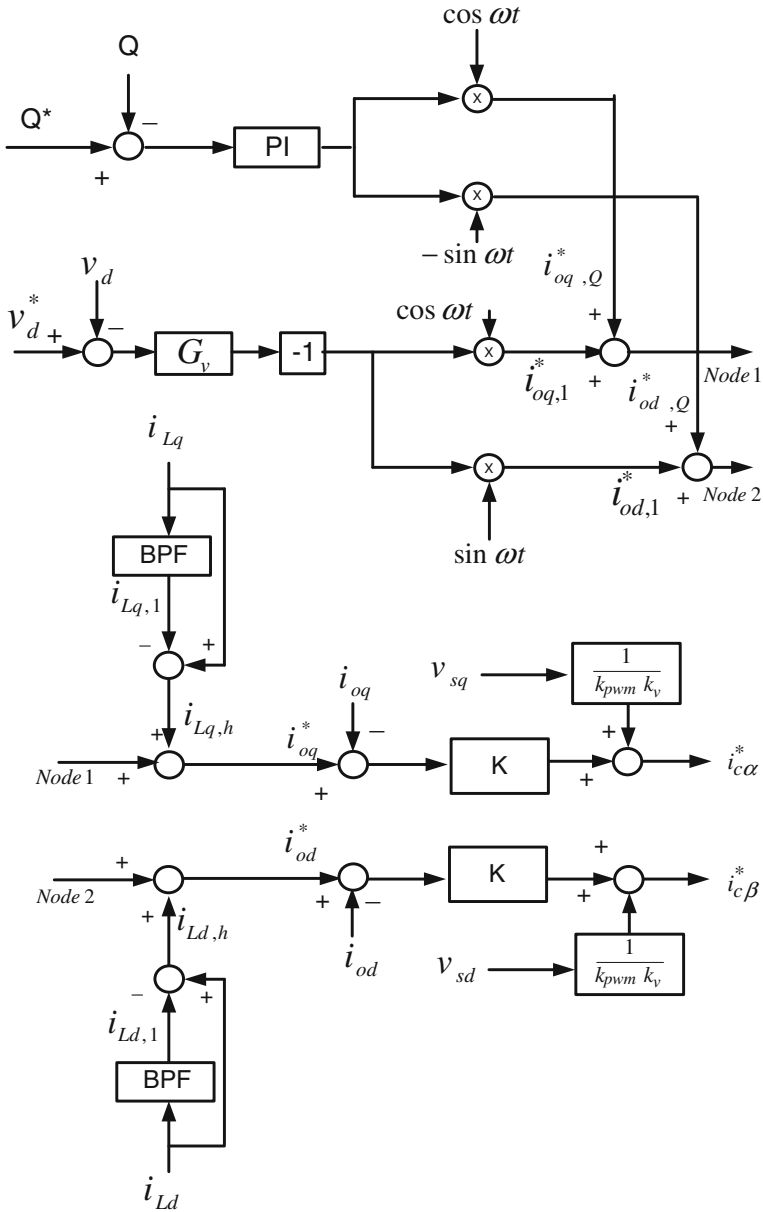
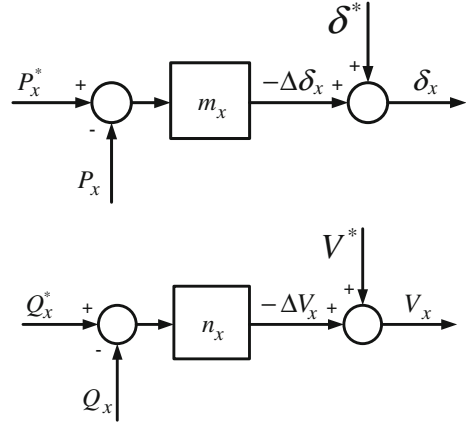


**Fig. 4** The signal block diagram of the derived HPIS controller

becomes simple for eliminating the high-frequency current harmonics. Besides, the typical advantages of PWM based current control method are its simplicity in implementation and the high speed of its current control loop. The block diagram of the

**Fig. 5** The signal block diagram of the adopted HPIS droop control controller



proposed current controller based on (4) is shown in Fig. 4. As can be seen from Fig. 4, the input commands to the derived controllers include three parts, i.e. the harmonic compensating current, the reactive power to be compensated, the DC voltage of the HPIS or the real power of the DG if desired. To achieve a better dynamic performance, a feed forward compensating path is also used. To compare dynamic control performances, another design approach on d-q reference frame is also investigated in this paper. Following the mathematical derivations presented previously in (2-4), the park's transformation can then be used to obtain the current control signals in d-q reference frame as expressed in (5). After some mathematical manipulations, the equivalent three-phase real and reactive power expressed in d-q reference frame can be expressed as (6). It is clear that the dc voltage on the capacitor in the HPIS can be achieved by regulating the real power (P) coming in and out of the three-phase inverter, while simultaneously control the output reactive power (Q) using the following equation (7) if desired. It follows that the three-phase current command signals for the proposed HPIS can be derived from (7) by using the inverse Park's and Clarke's transformations. To demonstrate the effectiveness of the proposed modular HPIS concept, the widely used droop control method shown in Fig. 5 is adopted for controlling the parallel connected HPIS inverters.

$$\begin{bmatrix} i_{od} \\ i_{oq} \end{bmatrix} = \begin{bmatrix} \cos \theta & -\sin \theta \\ \sin \theta & \cos \theta \end{bmatrix} \begin{bmatrix} i_{o\beta} \\ i_{o\alpha} \end{bmatrix} \quad (5)$$

$$\begin{bmatrix} P^{3-p} \\ Q^{3-p} \end{bmatrix} = \begin{bmatrix} \vec{i} & \vec{v} \\ \vec{i} & \vec{v} \\ \times \end{bmatrix} = \begin{bmatrix} v_d i_d + v_q i_q \\ v_d i_q - v_q i_d \end{bmatrix} \quad (6)$$

$$\begin{bmatrix} i_{od,P}^* \\ i_{oq,Q}^* \end{bmatrix} = \begin{bmatrix} i_d^* \\ i_q^* \end{bmatrix} = \begin{bmatrix} P/v_d \\ Q/v_d \end{bmatrix} \quad (7)$$



## 5 Case Studies and Results

To investigate the detailed dynamics of the proposed HPIS and to validate the proposed two control methods, comprehensive simulation studies are carried out on a MG distribution network connected with a nonlinear DG link in Matlab/Simulink environment. It is considered that for the whole period of simulations the local loads are fed by the main source of the micro-grid feeder. In this study, during the simulation active power which is delivered from DG link is assumed unlimited. This assumption makes it possible to evaluate the capability of HPIS to track the fast change in the harmonic currents and the reactive current components of the reactive power required by the load or the grid independently. To simulate a realistic operation scenario in micro-grid network, the nonlinear loads are connected and disconnected to MG distribution network and the harmonic distortion of current waveform are recorded and compared in various conditions. Since the principle of the proposed current control technique is based on separating active and reactive current components in two reference frames known as the two-axis components, in all conditions only phase-a parameters (voltage and current) are shown. To demonstrate the performance of the proposed modular HPIS to compensate total real and reactive power on variation of load, the R and R-L loads are tested and the output waveforms of the two HPIS modules are shown simultaneously. The switching frequency for the HPIS inverter is set at 20 kHz to achieve satisfactory response. In this study, the DC voltage is controlled at 400 V with the three-phase 220 V, 60 Hz power grid.

*Case-1: Connection of nonlinear load link to the MG feeder with the HPIS in operation*

In the first simulation case, the HPIS link is connected to the network at  $t = 0.0$  s. A nonlinear load is added to PCC and removed at  $t = 4.5$  s. Figure 6a and b respectively show the related current waveforms of the HPIS performing APF control functions with the proposed two control schemes. As can be seen in Fig. 6a with method-1 and b with method-2, after the connection of HPIS link to feeder (grid) the source current becomes sinusoidal since the harmonic currents are fully provided by the HPIS link. Based on the results shown in Fig. 6a and b, the HPIS link controlled with the proposed method-2 which is derived from the d–q reference frame has better dynamic performance. This is due to the fact that the method-2 with control signals derived from the d–q reference frame is able to eliminate the interactions in control signals between the two control loops for the real power and the reactive power.

*Case-2: Connection of the nonlinear load link to the MG feeder with two HPIS modules operated in droop control mode with the proposed d–q control scheme*

In this simulation case, two HPIS modules are connected to the network at  $t = 0.0$  s. A nonlinear load is also added to PCC at  $t = 0.0$  s. Two types of loads are arranged; i.e. the pure resistance load and the resistance plus inductance load. In all cases, at the simulation time instant of 0.3 s a step change in active and reactive load power are initiated. Figure 7a–e respectively show the related P-Q tracking results of the two HPIS modules. As can be seen in Fig. 7a an equal real power regulation

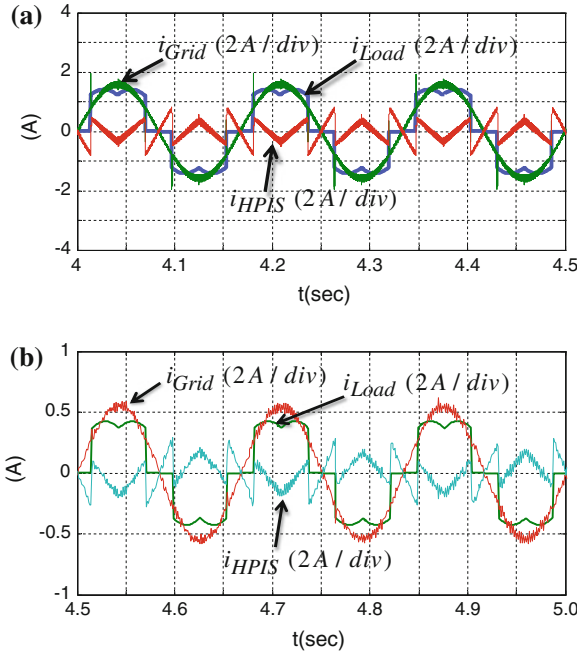


**Fig. 6** The related current waveforms in HPIS APF control functions. **a** Simulated results of the related current waveforms (method-1). **b** Simulated results of the related current waveforms (method-2)

result of the two HPIS inverters has been achieved; while the circulating reactive power between the two HPIS modules is negligible. Figure 7b shows the results of using different droop parameters of real power control. Figure 7c shows the results of using a set of identical droop parameters for both real and reactive power control. As can be seen from Fig. 7c both real and reactive powers are equally shared by the two HPIS modules. Figure 7d and e respectively show the results of using different droop parameters in real-power and reactive-power control loops.

## 6 Conclusion

This paper has demonstrated a novel design of a flexible hybrid power interface system in which any DG inverter system can be utilized as an APF for harmonic currents compensation and a reactive power generator for power factor correction and voltage control at the PCC. Based on the results obtained from the two simulation cases carried out in Matlab/Simulink software environment, the HPIS link with the proposed control schemes exhibits satisfactory functional and dynamic performances. The feasibility and effectiveness of the proposed modular HPIS and the droop control

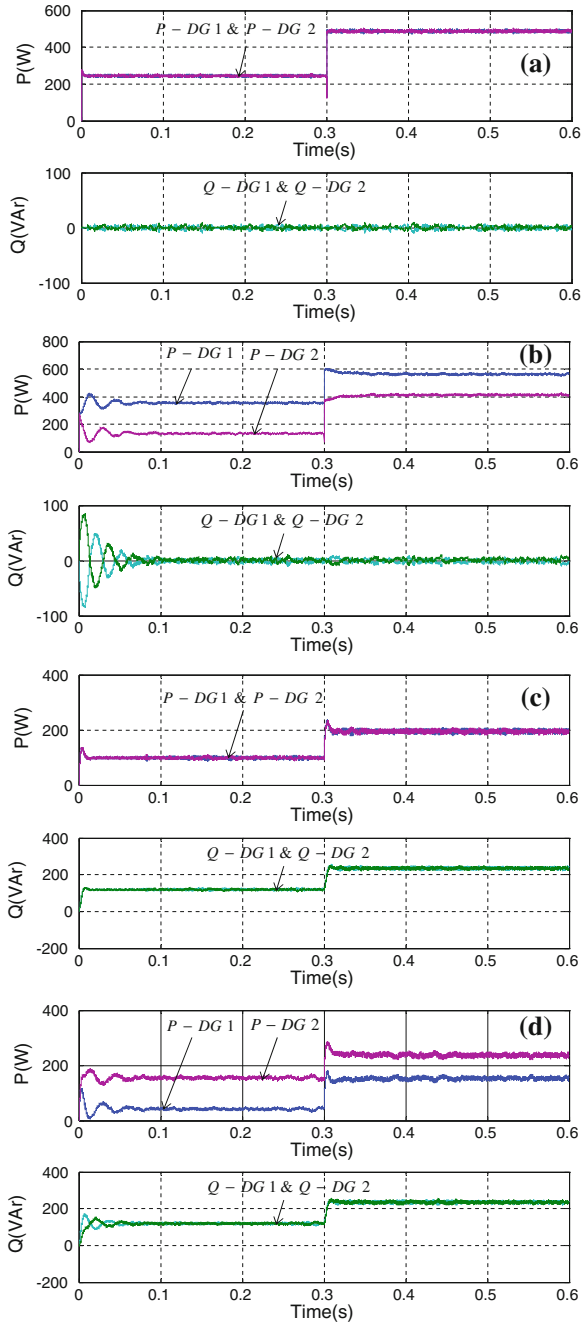


Fig. 7 The results of two HPIS modules operated in droop control mode

scheme have been confirmed. It is important to note that better dynamic response can be achieved if decoupled current controllers are used in the control loops of the HPIS.

**Acknowledgments** This work was supported in part by the National Science Council of Taiwan, R.O.C. through: NSC 101 - 2221-E -239-031.

## References

1. K.M. Syafii and M. A-A. Nor, Steady-State Wind Turbine Generation Model for Three-Phase Distribution Load Flow Analysis, IREMOS, Vol. 4 N. 2, April 2011 (Part B), pp. 772–777.
2. S. Arabi Nowdeh, B. Tousi, A. A. Zoraghchian and M. Hajibeigy, Optimal PV and FC Application in a Hybrid Power System with the Aim of Selling Electrical Energy to Distribution Network, IREMOS, Vol. 4 N. 5, October 2011(Part B), pp. 2392–2401.
3. Aghajani S, Joneidi IA, Kalantar M, Morteza pour V (February 2010) Modeling and Simulation of a PV/FC/UC Hybrid Energy System for Stand Alone Applications. IREMOS 3(1):82–89
4. Grubb M (1995) Renewable Energy Strategies for Europe, The Royal Institute of International Affairs, vol I. Foundations and Context, London, UK
5. Miyamoto Y, Hayashi Y (Oct. 2010) Evaluation of improved generation efficiency through residential PV voltage control of a clustered residential grid-interconnected PV. IEEE PES Innovative Smart Grid Technologies Conference Europe (ISGT Europe) 1:1–8
6. H. Laukamp, The new German electric safety standard for residential PV systems, The 25<sup>th</sup> IEEE Photovoltaic Specialists Conference, 13 May 1996, pp. 1405–1408.
7. J. Carr, J.C.Balda and A.Mantooth, A high frequency link multiport converter utility interface for renewable energy resources with integrated energy storage, Energy Conversion Congress and Exposition (ECCE), 12–16 Sept. 2010 IEEE, pp. 3541–3548.
8. IEEE Standard for Interconnecting Distributed Resources with Electric Power Systems, IEEE Standard 1547–2003, July 2003.
9. Varma RK, Khadkikar V, Seethapathy R (Dec. 2009) Nighttime Application of PV solar farm as STATCOM to Regulate Grid Voltage. IEEE Trans. Energy Conversion (Letters) 24(4):983–985
10. R.A. Mastromauro, M.Liserre, T.Kerekes and A.Dell’Aquila, A Single-Phase Voltage-Controlled Grid-Connected Photovoltaic System With Power Quality Conditioner Functionality, IEEE Transactions on Industrial Electronics, Vol. 56, Issue 11, 2009, pp. 4436–4444.
11. M. Anwari, M.I.M. Rashid and Taufik, Power quality analysis of grid-connected photovoltaic system with Adjustable Speed Drives, 2010 International Conference on Control Automation and Systems (ICCAS), 2010, pp. 2452–2456.
12. Majumder R, Ghosh A, Ledwich G, Zare F (2010) Power Management and Power Flow Control With Back-to-Back Converters in a Utility Connected Microgrid. IEEE Transactions on Power Systems 25(2):821–834
13. Chen C-L, Wang Y (2010) Jih-Sheng Lai, Yuang-Shung Lee and D. Martin, Design of Parallel Inverters for Smooth Mode Transfer Microgrid Applications, IEEE Transactions on Power Electronics 25(1):6–15
14. Nikkhajoei H, Lasseter RH (2009) Distributed Generation Interface to the CERTS Microgrid. IEEE Transactions on Power Delivery 24(3):1598–1608
15. R.H. Lasseter, A Akhil, C. Marnay, J Stephens, J Dagle, R Guttromson, A. Meliopoulos, R Yinger, and J. Eto, The CERTS Microgrid Concept, White Paper for Transmission Reliability Program, Office of Power Technologies, U.S. Department of, Energy, April 2002.
16. Tsao-Tsung Ma and Tzung-Han Shr, Design of a Cost-Effective Power Interface for Advanced Micro-grid Operation and Control, Lecture Notes in Engineering and Computer Science: Proceedings of The International Multi-Conference of Engineers and Computer Scientists 2013, 13–15 March, 2013, Hong Kong, pp 651–656.

17. Ma TT (November 2012) Yih-Der Lee, Yung-Ruei Chang and Chin-Lung Hsieh, "Advanced Operation and Control Schemes for a Micro-grid with Battery Energy Storage Systems". *International Journal of Advanced Renewable Energy Research*, Vo. 1(6):596–604
18. H. K. Høidalen and R. Sporild, Using Zigzag Transformers with Phase-shift to reduce Harmonics in AC-DC Systems, International Conference on Power Systems Transients (IPST'05) in Montreal, Canada, June 19–23, 2005, Paper No. IPST05 - 44.